Fabrication and electrical characterization of CdS quantum dots based solar cell

W. A. FAROOQ*, M. ATIF, F. YAKUPHANOGLU[a,b], AMANULLAH FATEHMULLA
Department of Physics and Astronomy, College of Science, King Saud University, P.O. Box 2455, Riyadh 11451, Saudi Arabia
[a]*Department of Physics, Faculty of Sciences Fırat University, Elazıg, Turkey*
[b]*Nanoscience and Nanotechnology Laboratory, Fırat University, Elazıg, Turkey*

A quantum dots sensitized solar cell was fabricated and the electrical characterizations of QDSSC were investigated. The solar cell gives a short circuit current density of 1.3mA/cm^2 and an open circuit voltage of 0.38V under AM1.5. The capacitance-voltage, conductance-voltage and series resistance-voltage characteristics of the solar cell were measured in a wide range of frequencies for the QDSSC application. The photovoltaic performance of the QDSSC can be improved using various chemicals.

(Received September 2, 2014; accepted April 5, 2016)

Keywords: Quantum Dot Sensitized Solar Cells (QDSSCs), Photovoltaic properties, Impedance spectroscopy

1. Introduction

There has been a growing concern on the research of photovoltaics over the past few decades due to the increased energy crisis and environment pollution. Apart from the p-n junction based solar cells many new types of solar cells such as dye- sensitized solar cells (DSSCs) and quantum dot sensitized solar cells also attract considerable interest. DSSC is a low cost cell and was first reported by Michael Gratzel and Brian O'Regan at the Ecole Ploytechnique Federal de Laussanne in 1991 [1-3].

In recent years, quantum dot (QD) sensitized solar cells have received a great attention due to their interesting properties such as low production cost and simple assemble technology [4–8]. The quantum dot size can control the optical band gap of photoanode material used in quantum dot sensitized solar cells to improve performance of the solar cell.

The various quantum dots from different materials have been used in quantum dot (QD) sensitized solar cell applications [9-13] to increase efficiency. In order to improve the efficiency of the solar cells, CdS quantum dot materials have been used by various researchers. The obtained results have indicated that CdS quantum dot is a promising material due to its suitable band gap (2.4 eV) to those of TiO_2 [14]. These quantum dots can be synthesized by successive ionic layer adsorption and reaction (SILAR) method.

In present work, we have prepared a Cadmium Sulphide (CdS) quantum dot solar cell and characterized the charge transport mechanism of the solar cell with capacitance-voltage and conductance –voltage measurements in a wide range of frequencies.

2. Experimental

TiO_2 coated fluorine doped tin oxide (FTO) glasses were purchased from Solaronix Co. Ltd and were used as photoanodes. The TiO_2 film was coated onto FTO glass and annealed at 500^{o}C. The CdS quantum dots were deposited on TiO_2 films by successive ionic layer deposition and reaction (SILAR) method. The solutions of 0.5 M $Cd(NO_3)_2$ in ethanol and 0.5 M Na_2S in methanol were prepared. The film was dipped into 0.5 M $Cd(NO_3)_2$ solution for 30 s and rinsed with ethanol and then, dipped into 0.5 M Na_2S for 30 s and rinsed with methanol. These dipping procedures are considered as one cycle. The coating procedure was repeated for 5 times. Platinum (Pt) deposited glass was used as a counter electrode. The polysulfide electrolyte was prepared using 0.5 M Na_2S, 2M and 0.2 M KCl. The active area of the solar cell was 0.36 cm^2. The contact for the electrode was made using a silver paste. The gold wire was attached to the electrodes. The current–voltage characteristics measurements were performed by using a KEITHLEY 4200 semiconductor characterization system. The photovoltaic measurements were taken using a Small-Area Class-BBA Solar Simulator and the light intensity was measured using a TM-206 solar power meter. All the measurements were done at room temperature. The surface morphology of TiO_2 nanostructure photo-electrode was studied by atomic force microscope (AFM) model: Park System, XE100 in a non-contact mode.

3. Results and discussion

3.1. Morphological characteristics

The surface morphology of TiO_2 thick film deposited on FTO, was studied using AFM and the confirmation of nanostructure of TiO_2 has already been reported in our earlier work elsewhere [15].

3.2. Photovoltaic characteristics of QDSSC

The current–voltage characteristics of the QDSSC were determined using a standard solar simulator. Fig. 1 represents the fourth quadrant of current-voltage characteristics. It can be observed from the experimental results of Fig.1 that both the photocurrent and photovoltage values indicate an increasing trend with the increasing illumination intensities. The short circuit current I_{sc} and open circuit voltage V_{oc} were observed to be 1.3mA/ cm^2 and 0.38 V respectively under 100 mW/ cm^2 illumination.

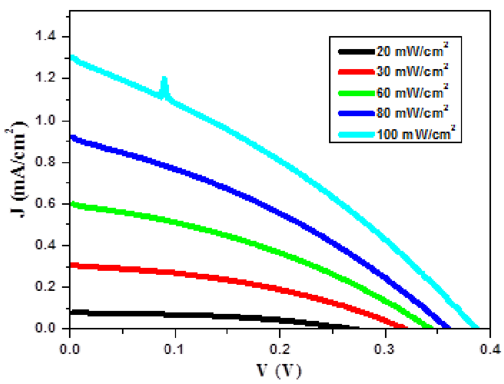

Fig. 1. Current-Voltage characteristics of QDSSC

The photovoltaic performance parameters (output power, open circuit voltage, short circuit current) against the incident light intensity of QDSSC are described. The plot of the electric power against voltage for QDSSC is shown in Fig. 2 indicating the delivered power to this device.

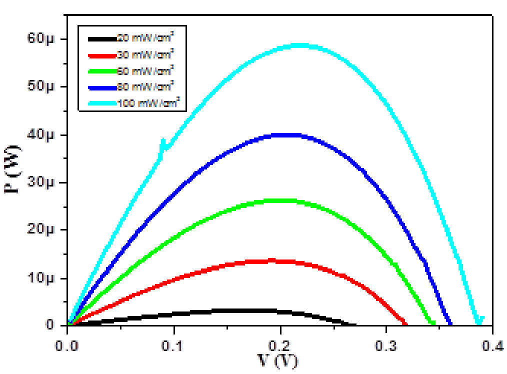

Fig. 2. Output power versus voltage curves for QDSSC

It is evident from the above figure (Fig. 2) that the electric power shows an increasing trend with the increasing bias voltage till it reaches its maximum power and later on decreases until reaches zero values with further increase of the applied voltage. The equation for the maximum power is given by:

$$P_{max} = I_m x V_m, \tag{1}$$

Where I_m shows the maximum current and V_m shows the maximum voltage at each illumination intensity. Hence the maximum power value shows how much the QDSSC can deliver its maximum power to an external load. From the figure 2, it is evident that the maximum power peak is shifted to the higher voltages with the increasing incident light as follows: 0.05 V, 1.5 μW at 20 mW/cm^2 and 0.22 V, 59μW at 100 mW/cm^2 respectively. We can observe the illumination dependence of the open circuit voltage in Fig. 3. The experimental results indicate that the value of V_{oc} increases with the light intensity until it attains a saturation value of 0.38 V.

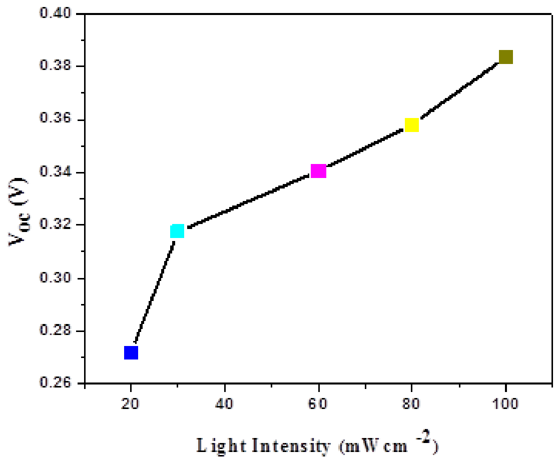

Fig. 3. Illumination dependence of the open circuit voltage V_{oc} for the QDSSC

From Fig. 3, it is evident that the photovoltaic voltage is almost proportional to the light intensity [16]. There is no major difference in DSSC and QDSSC except the replacement of dye with inorganic quantum dots. The working principle of QDSSC is almost same as that of DSSCs. The production of photocurrent in the QDSSC is due to absorption of the incident light throughout the quantum dots used as sensitized dye leading to ultra-fast electron injection in the conduction band of the TiO_2 [17-20]. It is observed that the movement of the injected electrons through the network of interconnected oxide particles is governed by a random path process [21] until they reach the conducting glass substrate.

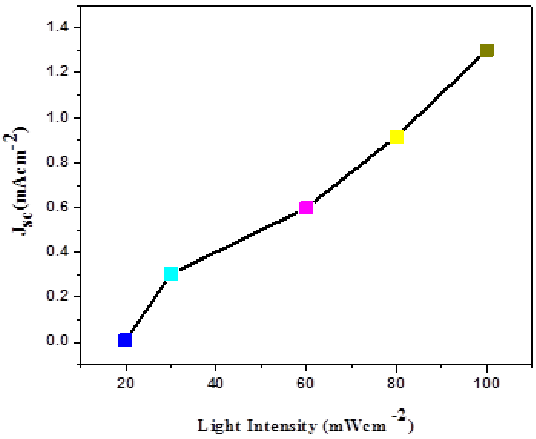

Fig. 4. Illumination dependence of the short circuit current J_{sc} for the nanostructured QDSSC

The experimental results show that both at lower and higher radiant power densities, the short circuit current J_{sc} tends to vary linearly with the power illumination representing that mass transport does not limit to the J_{sc} [22]. The short circuit current J_{sc} with open circuit voltage V_{oc} tends to vary as shown in Fig. 5. Hence it is concluded that with the increase of J_{sc} there is an increase in V_{oc} as well. We have observed from the curve fitting that there is a variation of V_{oc} with J_{sc} obeying the following relation [23-25]:

$$V_{oc} = \frac{nkT}{q}\ln\left(\frac{J_{sc}}{J_o}+1\right), \tag{2}$$

Where k is the Boltzmann's constant, q is the electric charge, n is the diode ideality factor, and J_0 is the reverse saturation current density. Eq.(2) shows V_{oc} is proportional to the log of J_{sc}. It is found that with increasing light intensity J_{sc} increases as shown in Figs.(4) and V_{oc} increases with increase of J_{sc} (Fig. 5) [24].

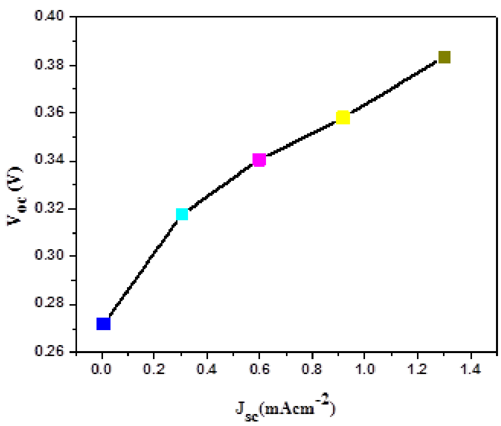

Fig. 5. The plot of short circuit current density J_{sc} as a function of open circuit voltage V_{oc} for the nanostructured QDSSC.

The efficiency of the cell is very low around 0.16% but the aim of this investigation is to study the effect of CdS QDS with SILAR method in QDSSC.

3.3. Impedance spectroscopy studies of QDSSC

Impedance spectroscopy studies include C-V and G-V characteristics. It is observed that Mott-Schottky equation for band bending in a single n-type semiconductor layer expresses the linear relationship between C^{-2}-V and is given by [26-28]:

$$\frac{1}{C_{SC}^2} = \left(\frac{2}{\varepsilon\varepsilon_o N_d e}\right)\left(V - V_{fb} - \frac{kT}{e}\right), \tag{3}$$

Where C_{SC} is the space charge capacitance of semiconductor electrode, ε is the dielectric constant of the semiconductor ε_0 is the permittivity of the free space, N_d is the dopant density, V is the applied potential and V_{fb} is the flat band potential. The Mott-Schottky ($1/C^2$versus V) plots are shown in Fig.6(a).We have found a deviation from linearity a good agreement with the results reported by Yin et al. [28] and this deviation is due to the effect of surface states, recombination effects, insufficient etching and non-negligible contributions of the Hemholtz layer to the interfacial capacitance. Hence Hemholtz layer capacitance can be described as the interface between metallic electrodes and an electrolyte solution behaving like capacitor and it has also a capability of storing electric charge [29].

At different frequencies, the capacitance-voltage characteristics for QDSSC are shown in Fig. 6 (b). It can be observed that with the change of bias voltage from -2 V to +2 V capacitance tend to vary slowly until it reaches its maximum value followed by a decrease in its values leading towards saturation with further increase of the bias voltage. Moreover with the increase of frequency from 10 kHz to 1 MHz the device capacitance demonstrates a decreasing behavior towards zero values. Further work is needed for the interpretation of these results.

With increasing frequencies from 10KHz to 1MHz at room temperature Conductance-Voltage (G-V) behavior for the QDSSC was also studied. The plots of conductance against bias voltage at different frequencies are shown in Fig. 7. The basis for this technique depends on the losses of conductance resulting from the exchange of majority carriers between interface states and majority carrier band of the semiconductor when a small ac signal is applied to the semiconductor devices [30]. From the experimental observations, it is clear that the conductance decreases with the increasing applied voltage from -2.0 to +2.0V and it is also found that the increase of the applied frequency results in the decrease of conductance. This is the result of the behavior of capacitance shift towards lower values at increased frequencies.

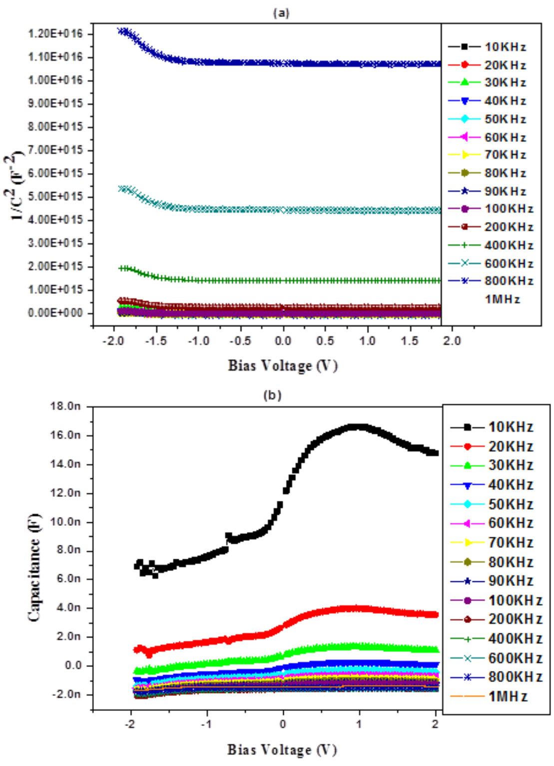

Figs. 6. (a) Mott-Schottky plot of the nanostructured QDSSC at different frequencies. (b) The capacitance profile as a function of biasing voltage at different frequencies for the nanostructured QDDSSC.

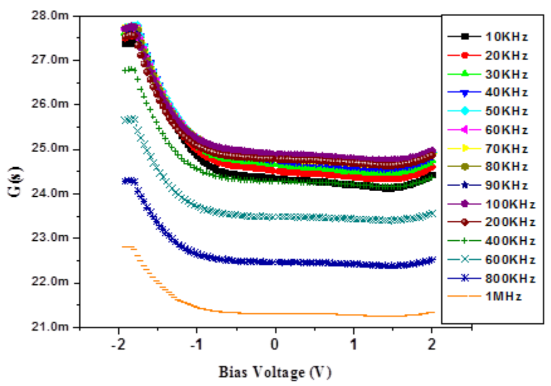

Fig. 7. Conductance-Voltage dependence of the nanostructured QDSSC at different frequencies.

4. Conclusions

For the preparation of Nano-structure of TiO_2 thick film on FTO glass, doctor blading technique is used. In this study we have investigated the photovoltaic properties (Current-Voltage) and impedance spectroscopy (Capacitance-Voltage and Conductance-Voltage) characteristics of nanostructured QDSSC. The experimental results of QDSSC show a short circuit current density of 1.3mA/cm^2 and an open circuit voltage of 0.38 V under AM 1.5. The mechanism of photovoltaic behavior of the solar cell is monitored with recombination. At different frequencies the capacitance–voltage characteristics of the device were examined by negative and positive bias voltages which show a decreasing trend of capacitance.

Acknowledgements

This work was supported by NPST program by King Saud University Project No. 11-NAN1464-02.

References

[1] B. O'Regan, M. Gratze, Nature **353**, 737 (1991).
[2] M. Gratzel, Nature **414**, 338 (2001).
[3] M. Gratzel, Inorg. Chem. **44**, 6841 (2005).
[4] J. Zhang, W. X. Que, Q. Y. Jia, P. Zhong, Y. L. Liao, X. D. Ye, Y. C. Ding, J. Alloys Compd. **509**, 7421 (2011).
[5] M. Grätzel, J. Photochem. Photobiol. A **164**, 3 (2004).
[6] C. S. Chou, R. Y. Yang, M. H. Weng, C. H. Yeh, Powder Technol. **187**, 181 (2008).
[7] C. S. Chou, Y. J. Lin, R. Y. Yang, K. H. Liu, Adv. Powder Technol. **22**, 31 (2011).
[8] B. O'Regan, M. Grätzel, Nature **353**, 737 (1991).
[9] N. Zhao, P. O. Tim, L. Y. Chang, M. G. Scott, D. Wanger, T. B. Maddalena, C. A. Alexi, G. B. Moungi, B. Vladimir, ACS Nano **4**, 3743 (2010).
[10] G. Serap, P. F. Karolina, N. Helmut, S. S. Niyazi, K. Sandeep, D. S. Gregory, Solar Energy Mater Solar Cells **91**, 420 (2007).
[11] J. Jiao, Z.-J. Zhou,W.-H. Zhou, S.-X. Wu, Materials Science in Semiconductor Processing **16**, 435 (2013).
[12] L. D. Wang, D. X. Zhao, Z. S. Su, D. Z. Shen, Nanoscale Res Lett **7**, 106 (2012).
[13] N. Zhou, G. P. Chen, X. L. Zhang, L. Y. Cheng, Y. H. Luo, D. M. Li, Q. B. Meng, Electrochem Commu **20**, 97 (2012).
[14] J. Li, L. Zhao, S. Wang, J. Hu, B. Dong, H. Lu, L. Wan, P. Wang, Materials Research Bulletin **48**, 2566 (2013).
[15] A. Fatehmulla, M. Atif, W. A. Farooq, M. Aslam, F. Yakuphanoglu, I. S. Yahia, Optoelectron. Adv. Mat. **8**(5-6), 587 (2014).
[16] S. J. Wu, C.-Y. Chen, J.-G. Chen, J.-Y. Li, Y.-L. Tung, K.-C. Ho, C.-G. Wu, Dyes Pigments **84**, 95 (2010).
[17] L. M. Peter, Dye-sensitized nanocrystalline solar cells, Phys. Chem. Chem. Phys. **9**, 2630 (2007).
[18] J. E. Moser, M. Wolf, F. Lenzmann, M. Gratzel, Z. Phys. Chem. **212**, 85 (1999).
[19] B. Burfeindt, C. Zimmermann, S. Ramakrishna, T. Hannappel, B. Meissner, W. Storck, F. Willig, Z. Phys. Chem. **212**, 85 (1999).
[20] Y. Tachibana, J. E. Moser, M. Gratzel, D. R. Klug, J. R. Durrant, J. Phys. Chem. **100**, 20056 (1996).
[21] Y. Wang, J. B. Asbury, T. Lian, J. Phys. Chem. A **104**, 4291 (2000).

[22] H. Wang, X. Liu, Z. Wang, H. Li, D. Li, Q. Meng, L. Chen, J. Phys. Chem. B **110**, 5970 (2006).
[23] M. L. Rosenblut, N. S. Lewis, J. Phys. Chem. **93**, 3735 (1989).
[24] A. Hagfeldt, H. Lindström, S. Södergren, S. E. Lindquist, J. Electroanal. Chem. **381**, 39 (1995).
[25] X. Sheng, Y. Zhao, J. Zhai, L. Jiang, D. Zhu, Appl. Phys. A **87**, 715 (2007).
[26] R. C. Kabir-ud-Din, M. A. Owen, Fox, J. Phys. Chem. **85**, 1679 (1981).
[27] J. Bandara, H. C. Weerasinghe, Sol. Energy Mater. Sol. Cells **88**, 341 (2005).
[28] X. Yin, W. Tan, J. Zhang, Y. Weng, X. Xiao, X. Zhou, X. Li, Y. Lin, Colloids Surf. A: Physicochem. Eng. Aspects **326**, 42 (2008).
[29] H. Helmholtz, Pogg. Ann. LXXXIX (1853) 211.
[30] E. H. Nicollian, A. Goetzberger, Appl. Phys. Lett. **7**, 216 (1965).

*Corresponding author: wafarooq@hotmail.com